Soil Biology & Biochemistry 109 (2017) 81–94

Contents lists available at ScienceDirect

Soil Biology & Biochemistry

journal homepage: www.elsevier.com/locate/soilbio

Combined turnover of carbon and soil aggregates using rare earth oxides and isotopically labelled carbon as tracers

Xinhua Peng [a, *], Qiaohong Zhu [a], Zhongbin Zhang [a], Paul D. Hallett [b]

[a] State Key Laboratory of Soil and Sustainable Agriculture, Institute of Soil Science, Chinese Academy of Sciences, Nanjing 210008, China
[b] Institute of Biological and Environmental Sciences, University of Aberdeen, Aberdeen AB24 3UU, UK

ARTICLE INFO

Article history:
Received 29 October 2016
Received in revised form
29 January 2017
Accepted 1 February 2017

Keywords:
Aggregate turnover
Modelling
Organic amendment
Rare earth oxide
Soil aggregation

ABSTRACT

This study used a combined tracer approach of isotopically labelled carbon (C) and rare earth oxides (REO) to determine soil aggregate transfer paths following input of organic matter. A model quantifying aggregate turnover rates over time was verified by a controlled incubation study. Four natural soil aggregate size ranges (<0.053 mm, 0.053–0.25 mm, 0.25–2 mm and 2–5 mm) were labelled with different REO tracers and packed to form a composite soil sample. The organic input was 1 mg $^{13}C\ g^{-1}$ soil of ^{13}C-labelled glucose. There were four treatments: i) soil without REO and ^{13}C as a control, ii) soil labelled with REO, iii) soil without REO but amended with ^{13}C-glucose, and iv) soil labelled with REO and amended with ^{13}C-glucose. Aggregate stability, REO concentrations, soil respiration and ^{13}C were measured after 0, 7, 14 and 28 days incubation. REOs were found to not impact microbial activity ($P > 0.05$). Based on the 84%–106% recovery of REOs after wet sieving of aggregates, and a close 1:1 relationship between measured aggregates and model predictions, REOs were found to be an effective tracer for studies of aggregate dynamics. A greater portion of aggregates transferred between neighbouring size fractions. The turnover rate was faster for macroaggregates than for microaggregates, and slowed down over the incubation time. The new C was accumulated more but decomposed faster in macroaggregates than in microaggregates. A positive relationship was observed between the ^{13}C concentration in aggregates and the aggregate turnover rate ($P < 0.05$). The relative change in each aggregate fraction generally followed an exponential growth over time in the formation direction and an exponential decay in the breakdown direction. We proposed a first order kinetic model for aggregate dynamics which can separate aggregate formation, stabilization and breakdown processes. This study demonstrates that REOs can track aggregate life cycles and provide unique and important information about the relationship between C cycling and aggregate turnover.

1. Introduction

Soil aggregate dynamics involves aggregate formation, stabilization and breakdown processes (Oades, 1993; Six et al., 2004), largely controlled by biological processes in soil (Tisdall and Oades, 1982) and their interaction with physical processes such as wetting/drying, thawing/freezing, and tillage (Le Bissonnais, 1996; Díaz-Zorita et al., 2002). Although considerable research has explored soil aggregate dynamics, the life cycle of an aggregate and its impact on microbial mediated C cycling remains elusive. This has been addressed to some extent by the use of particle tracers, which have been applied in a few studies of soil aggregate dynamics. Over the past three decades, a number of particle tracers have been employed such a 1–3 mm ceramic spheres (Staricka et al., 1992) or ≈500 μm Dy_2O_3 labelled ceramic prills (Plante et al., 1999; Plante and McGill, 2002a). Due to the size of the tracers, however, these studies were limited to macroaggregate dynamics.

Biological processes driving soil aggregation operate over a much broader range of scales, so smaller tracers are needed. Rare earth oxides (REO) were proposed by Zhang et al. (2001) to trace soil aggregation and erosion, and subsequently employed by De Gryze et al. (2006) to track aggregation dynamics of artificial aggregates. REOs are very small (<5 μm in diameter), easily detected, have strong binding energy with soil mineral surfaces and physicochemical properties similar to soil particles. The aim of De Gryze et al.'s (2006) study was to explore the transfer of soil between

* Corresponding author.
E-mail address: xhpeng@issas.ac.cn (X. Peng).

http://dx.doi.org/10.1016/j.soilbio.2017.02.002

different aggregate size fractions collected from wet sieving. REO concentrations detected much more rapid macroaggregate turnover than microaggregate turnover, and greater stabilization of soil in microaggregates. They also observed that REOs did not affect soil respiration, so could potentially be employed to investigate aggregate dynamics related to C cycling and inputs.

Modelling soil aggregate dynamics after organic matter input was reported in a few studies. Segoli et al. (2013) used data from De Gryze et al. (2006) to develop the AggModel that simulates macroaggregate and microaggregate dynamics. Another model of aggregate dynamics after organic input was the conceptual CAST model presented by Stamati et al. (2013). An earlier model by Kay et al. (1988) simulated aggregate formation and breakdown using first order kinetics, which they tested with previously published data of aggregate stability. De Gryze et al. (2005) also reported that an exponential equation fitted >2 mm aggregate dynamics data better than other equations. However, these four models did not disentangle the differences in aggregate formation, stabilization and breakdown processes. In contrast to a first order kinetic model, Monnier (1965) proposed a conceptual model that aggregate stability increases immediately after organic amendment and thereafter decreases as the organic matter decomposes. To examine the impact of quality of amended organic substances, Abiven et al. (2008) applied the Monnier's model to simulate changes in aggregate stability from four different organic inputs under controlled laboratory and field conditions. From a review of 48 sets of data published since the 1940s, Abiven et al. (2009) found no clear relationship between aggregate dynamics and organic matter decomposition. They argued that organic materials have different biochemical origins, direct abiotic impacts to aggregation, and varying impacts on aggregate breakdown mechanisms. Such complex processes driving how soil aggregates respond to the decomposition of organic matter and *vice versa* needs much more research.

A useful tool for such research could be REOs as tracers. In this study we develop the approach presented by De Gryze et al. (2006) and improve their model of incubation effect on soil aggregate turnover rate. To track biological transformation of C at the same time as aggregate turnover we employed a double-labelling approach with REOs to determine aggregate dynamics and ^{13}C-labelled glucose to determine new C distribution in aggregates. Our objectives were to propose a new method for labelling REO with natural aggregates and to develop a new model to determine aggregate turnover rate and time after organic input. This study will improve our understanding of the dynamics of soil aggregates and their feedback on C physical protection in soil. With current approaches, the understanding of soil aggregate, C dynamics and physical protection has been assembled from indirect assessments and the insightful interpretation of disparate data. Our new approach could trace pathways directly, providing hitherto unattainable, quantitative data to support a plethora of soil aggregation studies and soil C turnover modelling.

2. Materials and methods

2.1. The soil

The soil in this study was sampled from an arable field planted with peanut (*Arachis hypogaea* L.) at the Red Soil Ecological Experimental Research Station, Chinese Academy of Sciences (28°15′ N, 116° 55′ E), Yingtan, Jiangxi Province. The area has a typical warm and humid subtropical monsoon climate with an annual rainfall of 1795 mm and an annual mean temperature of 17.8 °C. The soil is derived from Quaternary red clay, classified as Acrisols (FAO, 2014), with mineralogy dominated by highly weathered 1:1 clays and iron oxides. Globally these soils are highly significant as they support food production for 40% of China's population, are commonplace in India and found in many other subtropical climates including Africa. The soil samples were collected from the surface 0–20 cm layer, air-dried and broken by hand to pass through a 5 mm sieve. Before imposing experimental treatments, the soil contained 7.50 g kg^{-1} soil organic C, −21.3‰ $\delta^{13}C$, 0.85 g kg^{-1} total N, and 38.9% clay content.

2.2. Rare earth oxides (REO) labelled aggregates

Four REOs (Lanthanum oxide, La_2O_3; Samarium oxide, Sm_2O_3; Neodymium oxide, Nd_2O_3 and Gadolinium oxide, Gd_2O_3) were purchased from Shanghai Heli Rare Earth Material Company, P.R. China. The purity of each oxide is >99.9%. The median diameter of the powder (D_{50}) ranged from 3.2 to 5.2 μm, and the density between 6.5 and 7.6 Mg m^{-3}. The background levels of the four REOs in the investigated soil were 2.59 mg kg^{-1} Gd_2O_3, 26.9 mg kg^{-1} La_2O_3, 5.35 mg kg^{-1} Sm_2O_3, 21.9 mg kg^{-1} Nd_2O_3.

Each REO tracer was added by wet mixing to a separate batch of bulk soil (<5 mm) at a rate of 500 mg kg^{-1}, in addition to a control without a tracer added. This involved first dispersing 3.33 mg ml^{-1} of REO in deionized water by vortex mixing. The soil was continuously mixed and sprayed slowly with the REO suspended in water at a rate of 150 ml kg^{-1} air dry soil. The initial sieving of the soil followed by spraying with an REO water suspension results in the preferential deposition of REOs on the surface of soil aggregates. The wetted soil was then stored at 4 °C for 7 days to allow water equilibration with minimal microbial activity. Afterwards, the soil was oven-dried at 40°C for 48 h, and broken down by hand to pass through a 5 mm sieve. The <5 mm soil was separated into four fractions by Elliott's (1986) method: large macroaggregates (2–5 mm), small macroaggregates (0.25–2 mm), microaggregates (0.053–0.25 mm), and silt and clay sized aggregates (<0.053 mm), indicated by A, B, C and D fractions, respectively. The fractioned aggregates were oven-dried at 40 °C and weighed.

Aggregates from A-D fractions were recombined into a soil in which each aggregate fraction contained a different REO tracer. One batch of bulk soil was mixed thoroughly for use in the REO labelling studies. The investigated soil was composed of A fraction labelled by Gd_2O_3 with 337 ± 8 mg kg^{-1}, B fraction labelled by La_2O_3 with 342 ± 8 mg kg^{-1}, C fraction labelled by Sm_2O_3 with 425 ± 9 mg kg^{-1}, and D fraction labelled by Nd_2O_3 with 577 ± 18 mg kg^{-1}. The protocol for combining four REO labelled aggregates into a soil is illustrated in Fig. 1. The control was subjected to the same procedure except without REO addition.

2.3. Soil incubation

Four treatments were designed as follows i) the soil without REO and ^{13}C as a control (Control treatment), ii) the soil labelled by REO (REO treatment), iii) the soil without REO but with added ^{13}C-glucose (^{13}C treatment), iv) the soil labelled with REO and added with ^{13}C-glucose (^{13}C + REO treatment). The treatments were established by placing 50 g soil in a 100 ml plastic bottle and amending with 7.5 ml ^{13}C-labelled glucose (99 atom% ^{13}C) for the ^{13}C and ^{13}C + REO treatments at an incorporation rate of 1.0 mg ^{13}C g^{-1} soil (equivalent to a glucose concentration in the added solution of 16.7 mg ml^{-1}). For the REO and Control treatments 7.5 ml of deionized water was added to the soil. Soils were then incubated for 28 days at 25°C with moisture kept at 60% water-holding capacity (0.15 g water g^{-1} soil) by regularly adding deionized water to maintain a constant weight. Aggregate dynamics were measured by destructively harvesting batches of soil on 0, 7, 14, and 28 day of

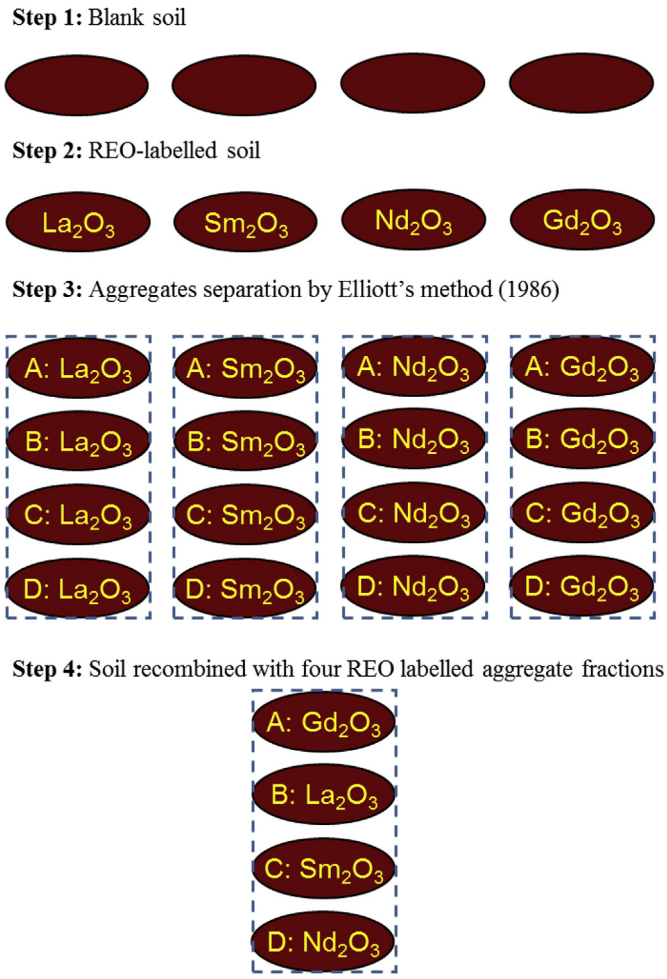

Fig. 1. The flow chart of the soil recombined by REO labelled four different aggregate fractions. A, B, C and D indicate 2–5 mm, 0.25–2 mm, 0.053–0.25 mm, and <0.0.53 mm aggregates, respectively.

incubation. At harvest soils were oven-dried at 40 °C for 48 h, and broken down <5 mm before measuring the aggregate size distribution, rare earth element and ^{13}C. All treatments were replicated 3 times.

2.4. Soil respiration

An additional three replicates of each treatment were used to measure soil respiration. The evolved CO_2 was trapped in 10 ml 1 M NaOH and back-titrated with 0.3 M HCl after the addition of 10 ml $BaCl_2$ solution (1 M) to precipitate to Na_2CO_3 (Zibilske, 1994). The traps were replaced periodically on 1, 3, 5, 7, 11, 14, 21, and 28 day of incubation. Air was renewed through replacement of the traps in each jar on each sampling date, thus maintaining aerobic conditions.

2.5. Aggregate fractionation

From the harvested soil sieved to <5 mm, water-stable aggregates were separated using the wet sieving method (Elliott, 1986). This involved placing 25 g of dry soil on a 2 mm sieve and submerging in deionized water for 5 min. The sieve was manually moved up and down by 3 cm, and this process was repeated 50 times over a 2 min period. The fraction remaining on the 2 mm sieve was collected in a pre-weighed aluminium pan. Water plus the filtered soil was poured through a 0.25 mm sieve, and the sieving procedure was repeated. Water plus the <0.25 mm fraction of soil was then poured through a 0.053 mm sieve, and the sieving procedure repeated. The remaining soil particles in the water were <0.053 mm. Each fraction was dried in an oven at 40 °C and weighed. Large macroaggregates (2–5 mm), small macroaggregates (0.25–2 mm), microaggregates (0.053–0.25 mm), and silt and clay sized aggregates (<0.053 mm) were obtained to determine the soil organic C (SOC), ^{13}C and REOs. The aggregate stability was calculated from the mean weight diameter (MWD) as:

$$\mathrm{MWD} = \sum_{i=1}^{n} \bar{x}_i \cdot w_i \quad (1)$$

where $\bar{x}_i$ is the mean diameter of each aggregate fraction, w_i is the mass proportion of aggregate fraction remaining on each sieve, and n is the number of fractions.

2.6. Rare earth oxide analysis

The contents of REOs were measured by ICP-MS after alkaline fusion (Bayon et al., 2009). Samples were prepared by pulverising REO labelled soil with an agate mortar and pestle to a fine powder. Afterwards, 125 mg of soil was placed into a corundum crucible, and mixed with 1 g Na_2O_2 and then covered by 0.25 g Na_2O_2. The crucible was put in a muffle furnace at 700 °C for 15 min. After cooling, the crucible was transferred into a beaker with 100 ml hot water. To remove the resulting H_2O_2 and complete co-precipitation, the beaker was heated to 200 °C on a hotplate for 3 h. The beaker was repeatedly washed with deionized water and 2% NaOH after keeping overnight. The precipitate was rinsed into a 250 ml volumetric flask with 2 drops of phenolphthalein indicator and dissolved by 1% HNO_3 to the colour change point. Another 2 ml HCl was added to the volumetric flask to maintain acidity. Then 15 ml sample solution was transferred into HDPE bottles and analysed for REOs by high resolution inductively coupled plasma mass spectrometry (HR-ICP-MS: Finnigan Element, USA).

2.7. ^{13}C concentration

The amount of ^{13}C in each aggregate fraction was measured with an EA-IRMS isotope ratio mass spectrometer (Thermo Finnigan, USA). The ^{13}C of the sample was expressed as follows (Chiang et al., 2004)

$$\delta^{13}\mathrm{C}(‰) = \left(\frac{R_{sample}}{R_{PDB}} - 1\right) \times 1000 \quad (2)$$

where R_{sample} and R_{PDB} is the $^{13}C/^{12}C$ ratio of the sample and the Pee Dee Belemnite (PDB) standard, respectively.

2.8. Recovery rate

The recovery rate (%) of glucose-derived ^{13}C or REO in all aggregates after incubation was calculated as:

$$\text{Recovery rate}(\%) = \sum_{i=1}^{n} \frac{\mathrm{Con}_j \times \mathrm{W}_i}{\mathrm{Soil}_j} \times 100 \quad (3)$$

where W_i is the mass of each aggregate fraction, n is the number of aggregate fractions, e.g., 2–5 mm, 0.25–2 mm, 0.053–0.25 mm, and <0.053 mm aggregates, j is the glucose-derived ^{13}C or REO, Con_j is the concentration of j in each aggregate fraction, and Soil_j is the amount of j in the soil. The REO concentration in Eq. (3) is after

subtracting its background in the soil or aggregate fraction.

2.9. Statistics analysis

Analysis of variance (ANOVA) using the whole data set was first performed at each sampling date to test the effects of REO addition, glucose-derived ^{13}C addition and their interaction on the measured variables (aggregate size distribution, aggregate stability (MWD), soil respiration, ^{13}C concentration, and aggregate turnover time) (SPSS, 2004). At a given treatment, an ANOVA was used to test the effect of sampling date on these variables. The least significant difference (LSD at $P < 0.05$) test was applied to assess the differences among the means of three replicates ($n = 3$). Pearson correlation test was performed to investigate relations between the aggregate turnover rate and the ^{13}C concentration in aggregates.

2.10. Mathematical description of aggregate turnover

A mathematical description of aggregate turnover by REO tracers was first reported by Plante et al. (2002), and then improved by De Gryze et al. (2006). However, Equation (15) in the study of De Gryze et al. (2006), which separates the recombination and incubation effects during aggregate turnover, has an error. In this study, we clarified the aggregate transform pathways and proposed a new equation for determining aggregate turnover that provides a new model of aggregate dynamics.

Our study tracked 4 different aggregate fractions (A-D, based on size), thereby producing 12 possible pathways with 6 potential break down pathways into smaller aggregates (*a-f*) and another other 6 (*g-l*) reformation pathways into larger aggregates (Fig. 2). These transfers between time t_1 and time t_2 can be summarized in a discrete transformation matrix $K(t_2\text{-}t_1)$:

$$K(t_2-t_1)=\begin{bmatrix} 1-a-d-f & g & j & l \\ a & 1-g-b-e & h & k \\ d & b & 1-j-h-c & i \\ f & e & c & 1-l-k-i \end{bmatrix} \quad (4)$$

where the $K(t_2\text{-}t_1)$ indicates the change in the proportions of aggregates falling into sizes A, B, C or D between time steps t_1 and t_2. The amount of aggregates at time steps t_1 and t_2 can be described by vectors $S(t_1)$ and $S(t_2)$:

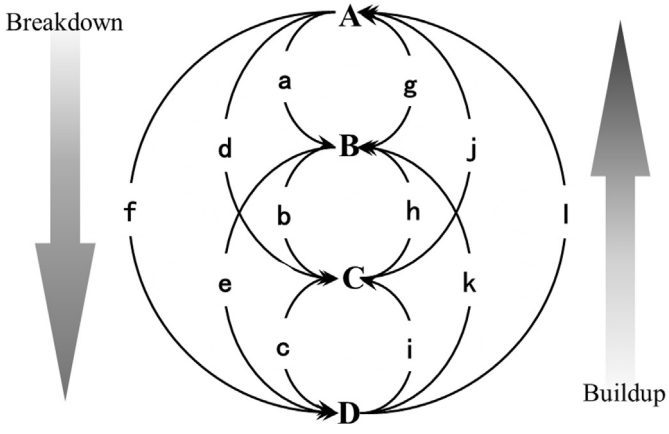

Fig. 2. The 12 possible pathways between four different aggregate fractions (*a-f* are breakdown direction and *g-l* are buildup direction). A, B, C and D indicate 2–5 mm, 0.25–2 mm, 0.053–0.25 mm and <0.053 mm, respectively.

$$S(t_1)=\begin{bmatrix} A(t_1) \\ B(t_1) \\ C(t_1) \\ D(t_1) \end{bmatrix} \quad (5)$$

$$S(t_2)=\begin{bmatrix} A(t_2) \\ B(t_2) \\ C(t_2) \\ D(t_2) \end{bmatrix} \quad (6)$$

where the A, B, C and D represent the amounts of large macroaggregates (2–5 mm), small macroaggregates (0.25–2 mm), microaggregates (0.053–0.25 mm), and silt and clay sized aggregates (<0.053 mm), respectively. When the mass conservation of aggregates is assumed during transfer between time steps t_1 and t_2, their relationship can then be described as follows:

$$S(t_2) = K(t_2 - t_1)S(t_1) \quad (7)$$

If the four aggregate fractions (A, B, C and D) in the $S(t_1)$ are labelled homogenously by the different REOs, and no loss of REOs are assumed during the aggregate fractionation procedure, the transformation matrix $K(t_2\text{-}t_1)$ in aggregates can be determined from the changes in REO amount between time steps t_1 and t_2. First, we gain the REO concentrations of different aggregate fractions at time t_1 as follows:

$$REO_{\text{con.}}(t)=\begin{bmatrix} [Gd_A] & [La_A] & [Sm_A] & [Nd_A] \\ [Gd_B] & [La_B] & [Sm_B] & [Nd_B] \\ [Gd_C] & [La_C] & [Sm_C] & [Nd_C] \\ [Gd_D] & [La_D] & [Sm_D] & [Nd_D] \end{bmatrix} \quad (8)$$

where, e.g., Gd_A is the concentration of Gd in large macroaggregate A fraction. The absolute REO amounts in the four aggregate fractions are:

$$REO_{\text{amo.}}(t)=\begin{bmatrix} A(t)[Gd_A] & A(t)[La_A] & A(t)[Sm_A] & A(t)[Nd_A] \\ B(t)[Gd_B] & B(t)[La_B] & B(t)[Sm_B] & B(t)[Nd_B] \\ C(t)[Gd_C] & C(t)[La_C] & C(t)[Sm_C] & C(t)[Nd_C] \\ D(t)[Gd_D] & D(t)[La_D] & D(t)[Sm_D] & D(t)[Nd_D] \end{bmatrix} \quad (9)$$

When the mass of REO is assumed to follow the mass conservation during aggregate transfers, Eq. (7) can be written as following:

$$REO_{\text{amo.}}(t_2) = K(t_2 - t_1)REO_{\text{amo.}}(t_1) \quad (10)$$

Consequently, the transformation matrix $K(t_2\text{-}t_1)$ can be calculated:

$$K(t_2 - t_1) = REO_{\text{amo.}}(t_2)REO_{\text{amo.}}(t_1)^{-1} \quad (11)$$

Since the soil is the mixture of four different aggregate fractions, aggregate transfers may happen during the recombination process at time t_1. The changes in REO concentrations in the soil after incubation between time steps t_2 and t_1 are ascribed to the recombination as an initial effect and the incubation effect. Thus, two discrete transformation matrices, one describing the effect of recombination prior to incubation, and the other describing the effect of recombination and the subsequent incubation, are used to calculate the effect of the incubation matrix:

$$K_{\text{inc}}(t_2 - t_1) = K_{\text{rec+inc}}(t_2) - K_{\text{rec}}(t_1) \quad (12)$$

where $K_{\text{rec+inc}}(t_2)$ is the discrete transformation matrix describing the effect of both recombination and incubation at time t_2, $K_{\text{rec}}(t_1)$ is

the discrete transformation matrix describing the effect of recombination prior to incubation at time t_1, and $K_{inc}(t_2\text{-}t_1)$ is the changes in discrete transformation matrix resulting only from the incubation effect from time step t_1 to t_2 (Eq. (13)).

$$K_{\mathrm{inc}}(t_2-t_1)=\begin{bmatrix} a_{t_1}+d_{t_1}+f_{t_1}-(a_{t_2}+d_{t_2}+f_{t_2}) & g_{t_2}-g_{t_1} & j_{t_2}-j_{t_1} & l_{t_2}-l_{t_1} \\ a_{t_2}-a_{t_1} & g_{t_1}+b_{t_1}+e_{t_1}-(g_{t_2}+b_{t_2}+e_{t_2}) & h_{t_2}-h_{t_1} & k_{t_2}-k_{t_1} \\ d_{t_2}-d_{t_1} & b_{t_2}-b_{t_1} & j_{t_1}+h_{t_1}+c_{t_1}-(j_{t_2}+h_{t_2}+c_{t_2}) & i_{t_2}-i_{t_1} \\ f_{t_2}-f_{t_1} & e_{t_2}-e_{t_1} & c_{t_2}-c_{t_1} & l_{t_1}+k_{t_1}+i_{t_1}-\left(l_{t_2}+k_{t_{2+i_{t_2}}}\right) \end{bmatrix} \quad (13)$$

In the aggregate breakdown (BD) direction, the changes in aggregate proportion of A, B and C fractions during the incubation from time t_1 to t_2 are expressed as follows:

$$\mathrm{BD(A)} = (a_{t_2} - a_{t_1}) + (d_{t_2} - d_{t_1}) + (f_{t_2} - f_{t_1}) \quad (14)$$

$$\mathrm{BD(B)} = (b_{t_2} - b_{t_1}) + (e_{t_2} - e_{t_1}) \quad (15)$$

$$\mathrm{BD(C)} = (c_{t_2} - c_{t_1}) \quad (16)$$

In the aggregate buildup (BU) direction, the changes in aggregate proportion of newly formed aggregates in A, B and C fractions during the incubation from time t_1 to t_2 are expressed as following:

$$\mathrm{BU(A)} = \frac{(g_{t_2} - g_{t_1})B(t_1) + (j_{t_2} - j_{t_1})C(t_1) + (l_{t_2} - l_{t_1})D(t_1)}{A(t_1)} \quad (17)$$

$$\mathrm{BU(B)} = \frac{(h_{t_2} - h_{t_1})C(t_1) + (k_{t_2} - k_{t_1})D(t_1)}{B(t_1)} \quad (18)$$

$$\mathrm{BU(C)} = \frac{(i_{t_2} - i_{t_1})D(t_1)}{C(t_1)} \quad (19)$$

In the aggregate breakdown direction, if the BD > 0, this fraction undergoes a destabilization process over time; if the BD < 0, this fraction undergoes a stabilization process over time. In the aggregate formation direction, the BU is always greater than 0. The aggregate D fraction (<0.053 mm) could not be taken into account in the breakdown and formation processes because no fraction smaller than fraction D was investigated in this study.

The turnover rate (TR) of each aggregate fraction (A, B, C and D) during incubation from time t_1 to t_2 is expressed as following:

$$\mathrm{TR(A)} = \frac{|a_{t_1} + d_{t_1} + f_{t_1} - (a_{t_2} + d_{t_2} + f_{t_2})|}{t_2 - t_1} \quad (20)$$

$$\mathrm{TR(B)} = \frac{|g_{t_1} + b_{t_1} + e_{t_1} - (g_{t_2} + b_{t_2} + e_{t_2})|}{t_2 - t_1} \quad (21)$$

$$\mathrm{TR(C)} = \frac{|j_{t_1} + h_{t_1} + c_{t_1} - (j_{t_2} + h_{t_2} + c_{t_2})|}{t_2 - t_1} \quad (22)$$

$$\mathrm{TR(D)} = \frac{|l_{t_1} + k_{t_1} + i_{t_1} - (l_{t_2} + k_{t_2} + i_{t_2})|}{t_2 - t_1} \quad (23)$$

The turnover time of this aggregate fraction is the reciprocal of its turnover rate. The turnover rate is assumed to be the first order kinetic, which was also suggested by Plante and McGill (2002a):

$$\frac{dy}{dt} = Me^{-rt} \quad (24)$$

where M is the change in aggregate proportion at a given fraction at time $t = 0$, and r is the parameter describing the relationship between turnover rate and time. Integrating Eq. (24) from time step $t = 0$ to time t yields:

$$y(\mathrm{t}) = \frac{M}{r(1 - e^{-rt})} \quad (25)$$

where $\frac{M}{r}$ is the total change in aggregate proportion at a given fraction at time $t = \infty$.

3. Results

3.1. REO recovery and its impact on microbial activity

The recovery rates of the four REOs ranged from 84% to 106% on the four sampling dates over the 28 days incubation (Table 1). The averaged recovery rate was 99% and 98% for Gd_2O_3 in REO and ^{13}C + REO treatments, respectively, and 97% and 100% for La_2O_3, greater than those for Sm_2O_3 (94.8–95.3%) and Nd_2O_3 (93–96%). The glucose addition did not impact the recovery rate of the REOs ($P > 0.05$).

REOs did not affect microbial activity as indicated by soil respiration (Fig. 3). The greatest respiration was on day 1, and decreased rapidly over the following days. It was not surprising that the addition of glucose enhanced respiration remarkably ($P < 0.001$). After 28 days incubation, the cumulative respiration was 1394 mg CO_2-C kg^{-1} soil for the ^{13}C treatment, 1343 mg CO_2-C kg^{-1} soil for the ^{13}C + REO treatment, 203 mg CO_2-C kg^{-1} soil for the Control treatment and 189 mg CO_2-C kg^{-1} soil for the REO treatment.

3.2. Aggregate size distribution

The effects of incubation time, REO and glucose addition on aggregate size distribution are displayed in Fig. 4. Prior to incubation (day 0), the 2–5 mm, 0.25–2 mm, 0.53–0.25 mm and <0.53 mm aggregates comprised 1.7%, 24.7%, 43.6% and 30.0% of the total soil mass, respectively. In the Control treatment, a slight increase from 3.6% on day 7 to 4.8% on day 28 was observed for 2–5 mm aggregates but the changes in other aggregate size fractions were minor. Relative to the Control treatment, the addition of REO alone did not change the proportions of the 2–5 mm aggregates ($P > 0.05$), but decreased 0.25–2 mm and 0.053–0.25 mm aggregates significantly ($P < 0.05$), and increased <0.053 mm

Table 1
Recovery of rare earth oxides (REO) after 0, 7, 14 and 28 day incubation.

Incubation time	REO				^{13}C + REO			
	Gd	La	Sm	Nd	Gd	La	Sm	Nd
0 d	97 ± 1	96 ± 2	90 ± 6	85 ± 2	97 ± 1	96 ± 2	90 ± 6	85 ± 2
7 d	98 ± 5	91 ± 2	87 ± 1	84 ± 7	99 ± 3	98 ± 2	93 ± 3	95 ± 3
14 d	102 ± 1	99 ± 8	105 ± 4	103 ± 2	96 ± 4	106 ± 5	101 ± 5	104 ± 6
28 d	99 ± 3	100 ± 3	97 ± 3	98 ± 2	99 ± 2	100 ± 3	97 ± 1	100 ± 1

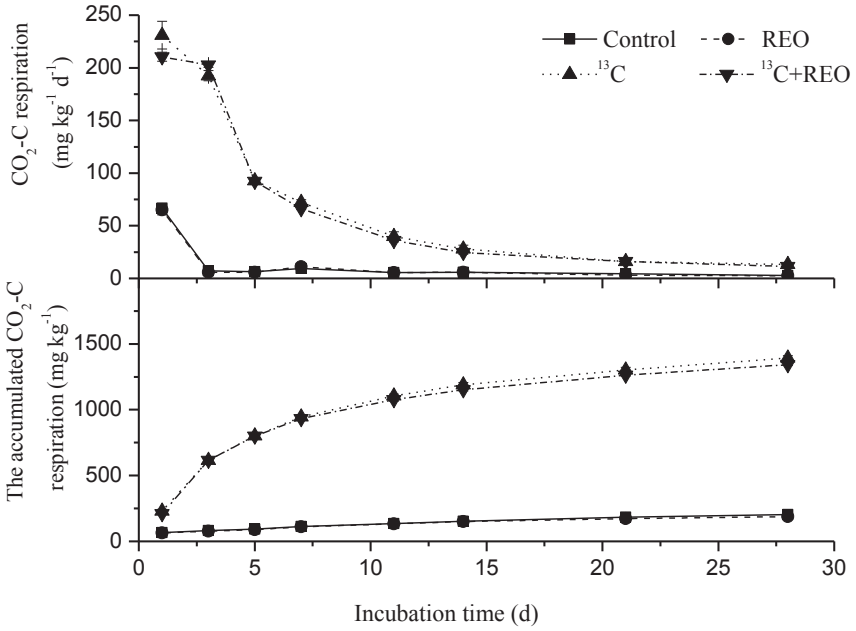

Fig. 3. The daily and accumulated soil respiration over 28-day incubation under treatments of i) soil without REO and ^{13}C as a control, ii) soil labelled with REO, iii) soil without REO but amended with ^{13}C-glucose, and iv) soil labelled with REO and amended with ^{13}C-glucose.

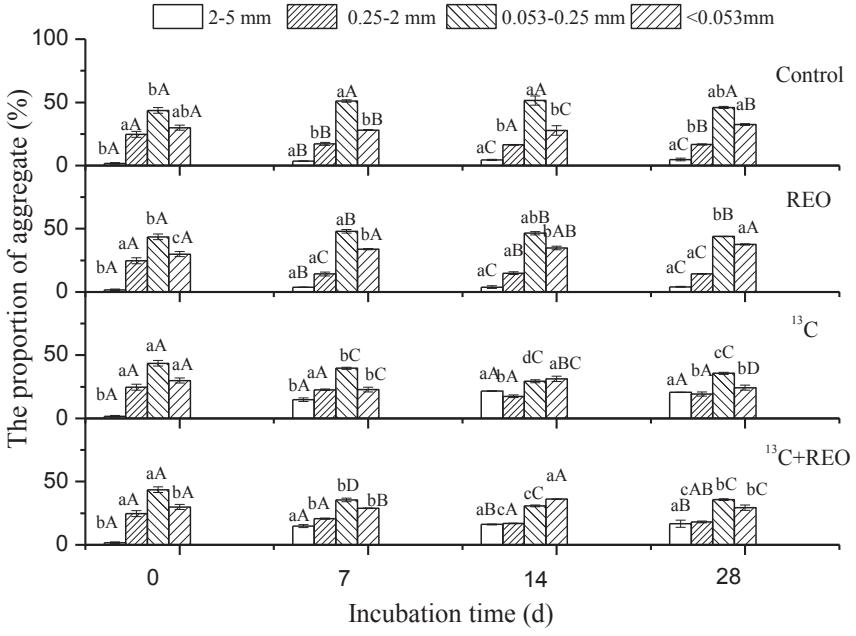

Fig. 4. The proportion of four aggregate fractions on 0, 7, 14 and 28 days of incubation under treatments of i) soil without REO and ^{13}C as a control, ii) soil labelled with REO, iii) soil without REO but amended with ^{13}C-glucose, and iv) soil labelled with REO and amended with ^{13}C-glucose. Different lowercase letters denote significant differences at $P < 0.05$ between sampling dates under the same treatment ($P < 0.05$) and different captical letters denote significant differences at $P < 0.05$ between treatments on the same sampling date.

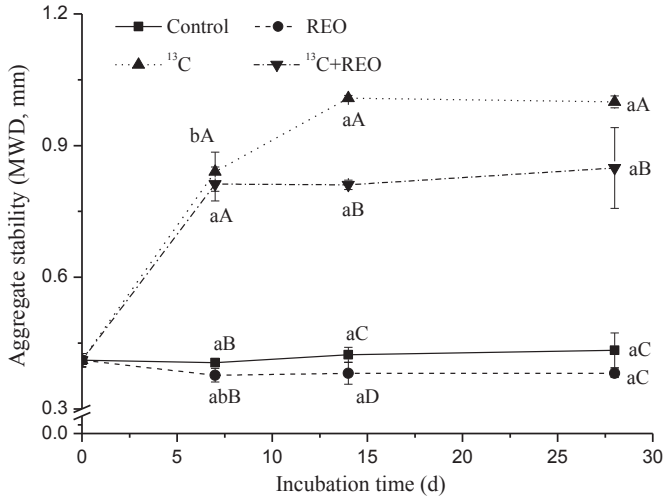

Fig. 5. The dynamics of aggregate stability (MWD) over time under i) soil without REO and ^{13}C as a control, ii) soil labelled with REO, iii) soil without REO but amended with ^{13}C-glucose, and iv) soil labelled with REO and amended with ^{13}C-glucose over incubation time. Different lowercase letters denote significant differences at P < 0.05 between sampling dates under the same treatment ($P < 0.05$), and different captical letters denote significant differences at $P < 0.05$ between treatments on the same sampling date.

aggregates ($P < 0.05$). The addition of glucose increased the proportion of 2–5 mm and 0.25–2 mm aggregates considerably ($P < 0.05$) at the expense of <0.25 mm aggregates ($P < 0.05$) (^{13}C *vs* Control, ^{13}C + REO *vs* REO). In the presence of a REO, the efficiency of glucose addition on >0.25 mm aggregation was less than for the glucose treatment alone after one week incubation ($P < 0.05$).

Aggregate stability increased from its initial value (MWD = 0.41 mm) for glucose amended soil ($P < 0.001$), but not for the Control or REO treatments over the incubation time (Fig. 5). The greatest increase in MWD was observed in the first week after the incorporation of glucose into the soil. The aggregate stability showed no difference on day 7 incubation between the ^{13}C + REO and ^{13}C treatments, but decreased significantly later on in the ^{13}C + REO treatment relative to the ^{13}C treatment ($P < 0.01$). The MWD in all treatments showed no difference between day 14 and day 28 incubation ($P > 0.05$). An interaction between REO and glucose amendment was only observed for day 14 ($P < 0.001$).

3.3. ^{13}C distribution in aggregates

The ^{13}C concentration decreased from 0.64–0.65 mg g^{-1} on day 7 to 0.35–0.44 mg g^{-1} on day 28 due to C mineralization (Fig. 6). The wet sieving for aggregate fractionation further lost 0.02–0.12 mg ^{13}C g^{-1} soil, but the recovery of ^{13}C after wet sieving increased with incubation time from 81 to 83% on day 7 up to 85–96% on day 28. The REO did not affect the new ^{13}C accumulation in the first two weeks of incubation, e.g., 0.65 *vs* 0.64 C mg g^{-1} on day 7, and 0.59 *vs* 0.59 C mg g^{-1} on day 14 in the ^{13}C and ^{13}C + REO treatments, respectively. On day 28, however, the presence of REO decreased ^{13}C concentration in the soil by 0.05 C mg g^{-1} and decreased ^{13}C recovery (85%) after wet sieving, relative to the glucose addition only (96%).

New ^{13}C accumulated more in >0.25 mm macroaggregates than in <0.25 mm aggregates, and the difference among aggregate fractions declined with incubation time (Fig. 7). On day 7, a greater concentration of ^{13}C was observed in >0.25 mm macroaggregates in the glucose treatment (0.68 mg C g^{-1}) and in the ^{13}C + REO treatment (0.65 mg C g^{-1}). With increasing incubation time, the ^{13}C concentration in macroaggregates decreased to 0.39–0.53 mg C g^{-1} on day 28. However, smaller changes were observed for 0.053–0.25 mm and <0.053 mm aggregates from 0.42–0.47 to 0.40–0.43 mg C g^{-1} in the ^{13}C treatment and to 0.27–0.31 mg C g^{-1} in the ^{13}C + REO treatment. The ^{13}C concentration in <0.053 mm aggregates was nearly constant (0.42 *vs* 0.43 mg C g^{-1}) over the incubation period in the ^{13}C treatment. For ^{13}C and ^{13}C + REO treatments the decrease of ^{13}C concentration from day 7 to day 28 incubation was greatest for aggregates of size 0.25–2 mm (0.25 mg C g^{-1}), followed by 2–5 mm (0.15 mg C g^{-1}),

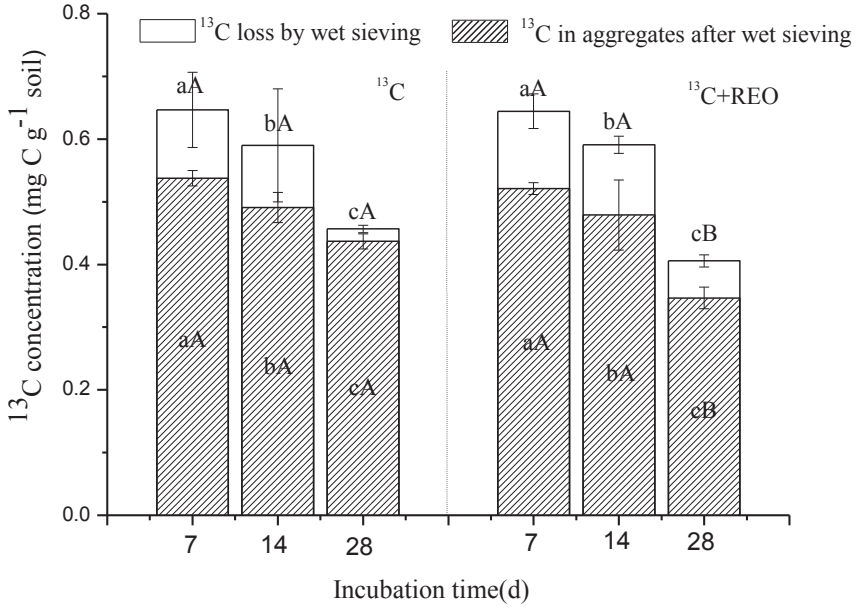

Fig. 6. The concentration of ^{13}C-glucose in aggregates and the loss by wet sieving without (^{13}C treatment) and with REO addition (^{13}C + REO). Different lowercase letters denote significant differences at P < 0.05 between sampling dates under the same treatment ($P < 0.05$), and different captical letters denote significant differences at $P < 0.05$ between treatments on the same sampling date.

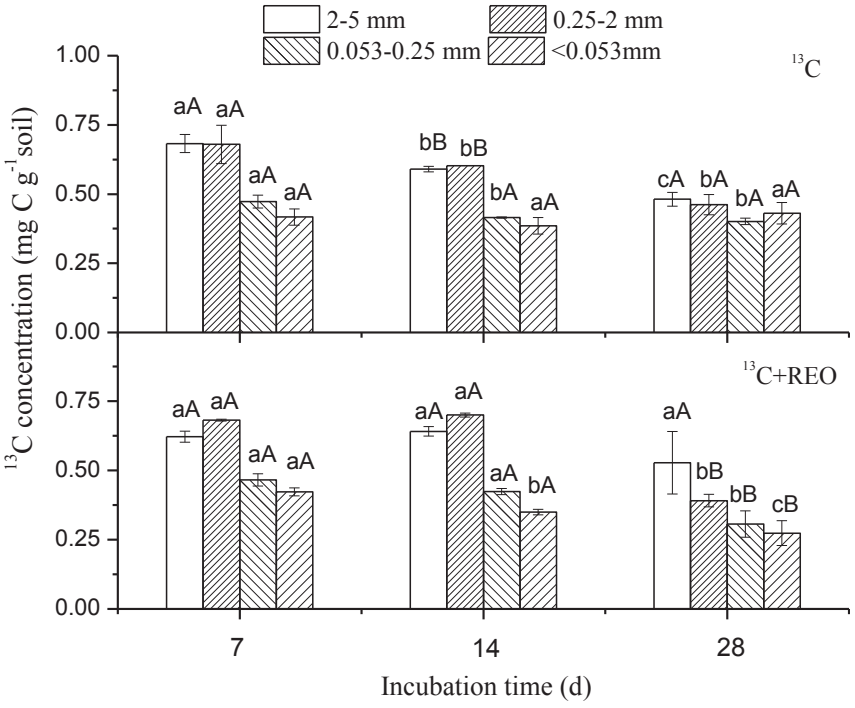

Fig. 7. The distribution of ^{13}C-glucose in soil aggregate fractions during incubation. Different lowercase letters denote significant differences at $P < 0.05$ between sampling dates under the same treatment, and different captical letters denote significant differences at $P < 0.05$ between treatments on the same sampling date.

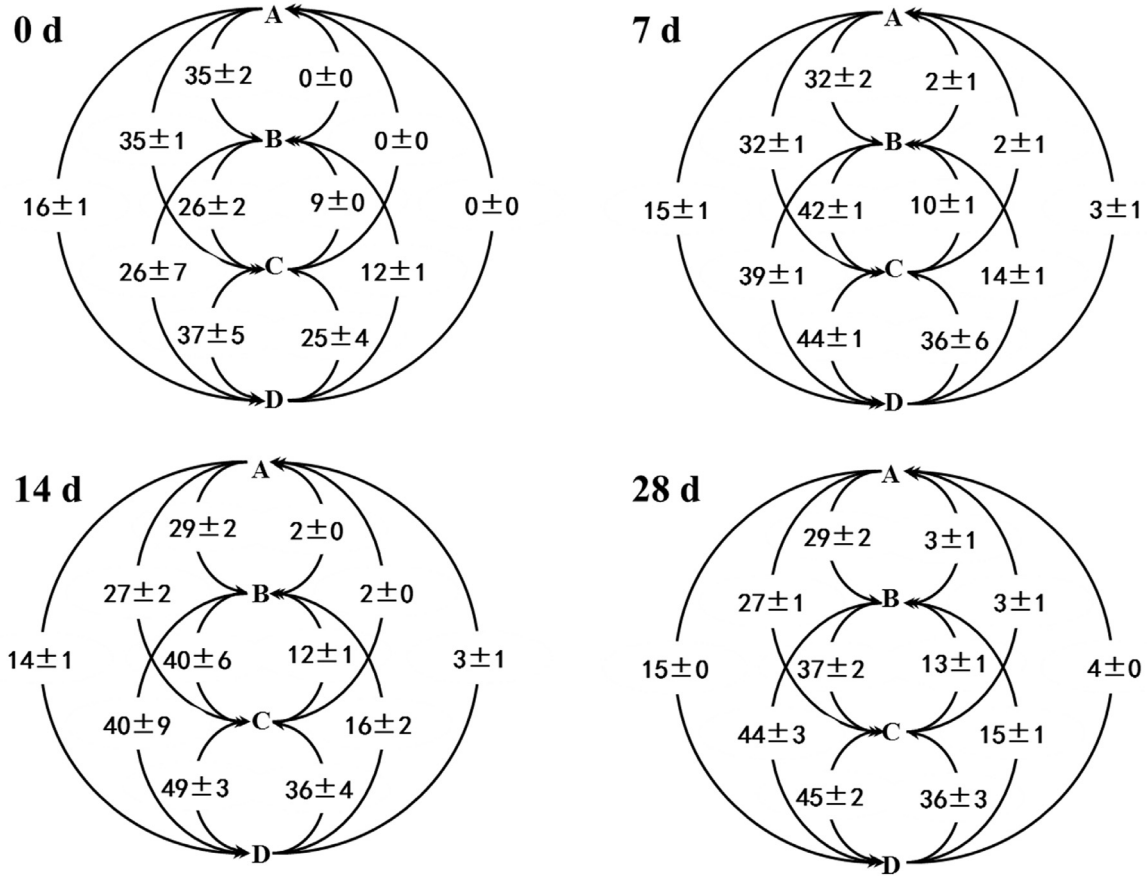

Fig. 8. The 12 transformation paths of four aggregate fractions on 0, 7, 14 and 28 day of incubation under the REO treatment. Values in arrows are the relative change of this aggregate fraction (%). A, B, C, and D represent 2–5 mm, 0.25–2 mm, 0.053–0.25 mm, and <0.053 mm aggregates, respectively.

0.053–0.25 mm (0.12 mg C g^{-1}), and <0.053 mm (0.07 mg C g^{-1}). Relative to the ^{13}C treatment, the REO addition did not change the ^{13}C concentration on day 7 but reduced its concentration for <2 mm aggregates significantly ($P < 0.05$) on day 28.

3.4. Aggregate transformation paths

The transfer paths among the four aggregate size fractions were calculated by the changes in the REO amount (Figs. 8 and 9). On day 0, the changes in aggregate fractions were resulted from the recombination and wet sieving effect. The larger the aggregate size fraction, the greater was the change due to the recombination and the wet sieving effect. Relative to day 0, the differences in transfer paths on day 7, 14 and 28 were caused by the incubation effect using Eq. (12). The changes in either breakdown or formation directions mainly happened in the first week, and then became less over the incubation time. A greater transfer portion of soil aggregates was observed between neighbouring size fractions either in breakdown or formation directions. The glucose addition significantly reduced aggregate breakdown ($P < 0.001$) and increased aggregate formation ($P < 0.001$). Relative to the REO treatment, 2–5 mm, 0.25–2 mm and 0.053–2 mm aggregates showed a less breakdown in the ^{13}C + REO treatment by 36–38%, 10–18% and 3–9%, respectively, indicating that the glucose addition stabilized larger aggregates greater than smaller ones.

To test the efficacy of REOs as tracers for aggregates transformation, the amount of aggregates was predicted using Eq. (7) according to the REO transfer matrix shown in Figs. 8 and 9. The relationships between the measured aggregates versus the predicted aggregates for the four fractions were close to the 1:1 line ($P < 0.001$) (Fig. 10). The slope of the regression was close to 1 for 2–5 mm and 0.25–2 mm aggregates ($P < 0.001$). However, it was smaller than 1 for the 0.053–0.25 mm fraction, and greater than 1.0 for the <0.053 mm fraction.

3.5. Aggregate turnover

The aggregate turnover rate decreased exponentially over the incubation time (Supplementary Material Table S1). In most of the fractions this can be described by the first order kinetic model (Equation (25)), although only four sampling dates were available. The glucose addition significantly improved the aggregate turnover rate in which greater was observed for 2–5 mm aggregates. A significantly linear relationship was observed between the turnover rate and ^{13}C concentration in aggregates ($P < 0.05$) (Fig. 12).

The aggregate turnover time, reciprocal to the aggregate turnover rate, increased with the incubation time, and the glucose addition decreased the turnover time significantly except for the 0.25–2 mm aggregates (Table 2). During the 28 day incubation, the shortest turnover time was observed for 0.25–2 mm aggregates (87 days) in the REO treatment and for 2–5 mm aggregates (54 days) in the ^{13}C + REO treatment, while the longest turnover time was observed for 0.053–0.25 mm aggregates from the REO treatment (186 days) and the ^{13}C + REO treatment (130 days).

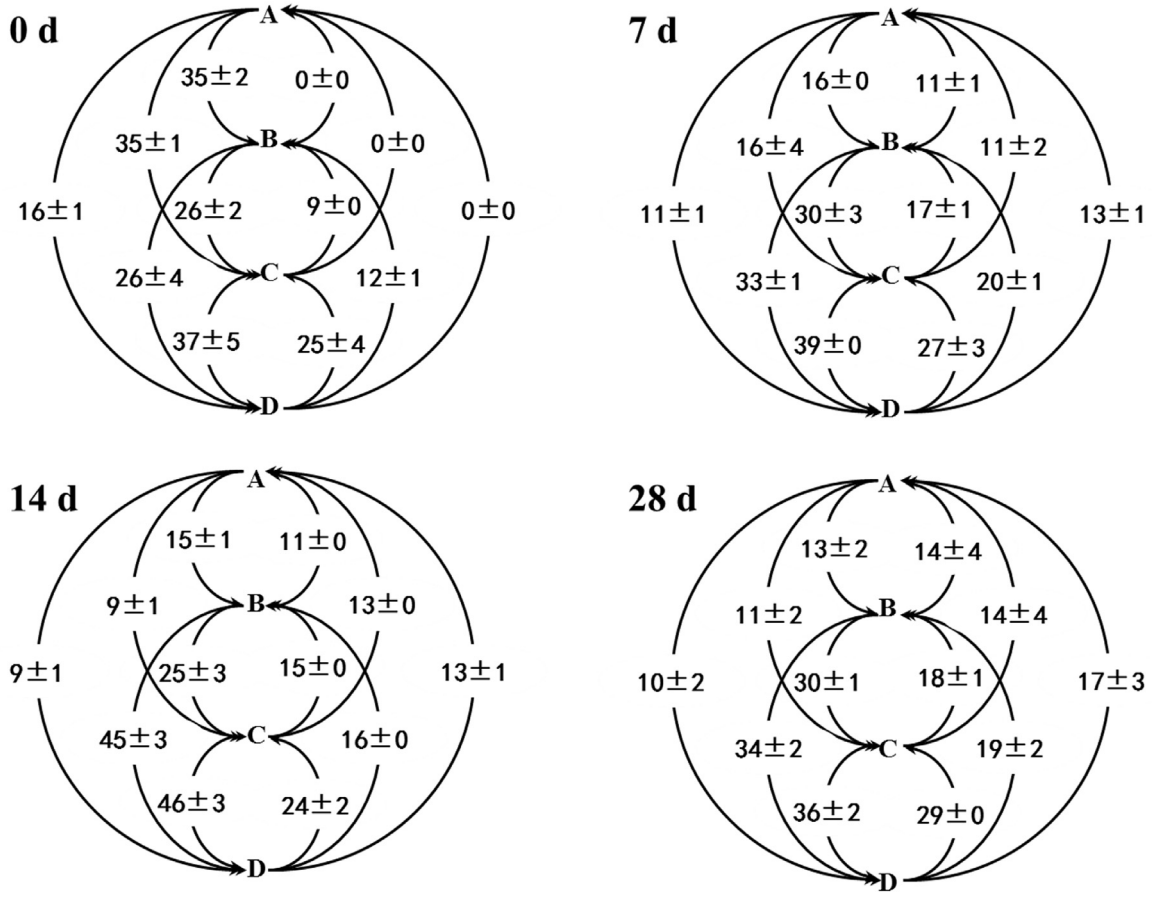

Fig. 9. The 12 transformation paths of the proportions of four aggregates on 0, 7, 14 and 28 day of incubation under the ^{13}C + REO treatment. Values in arrows are the relative change of this aggregate fraction (%). A, B, C, and D represent 2–5 mm, 0.25–2 mm, 0.053–0.25 mm, and <0.053 mm aggregates, respectively.

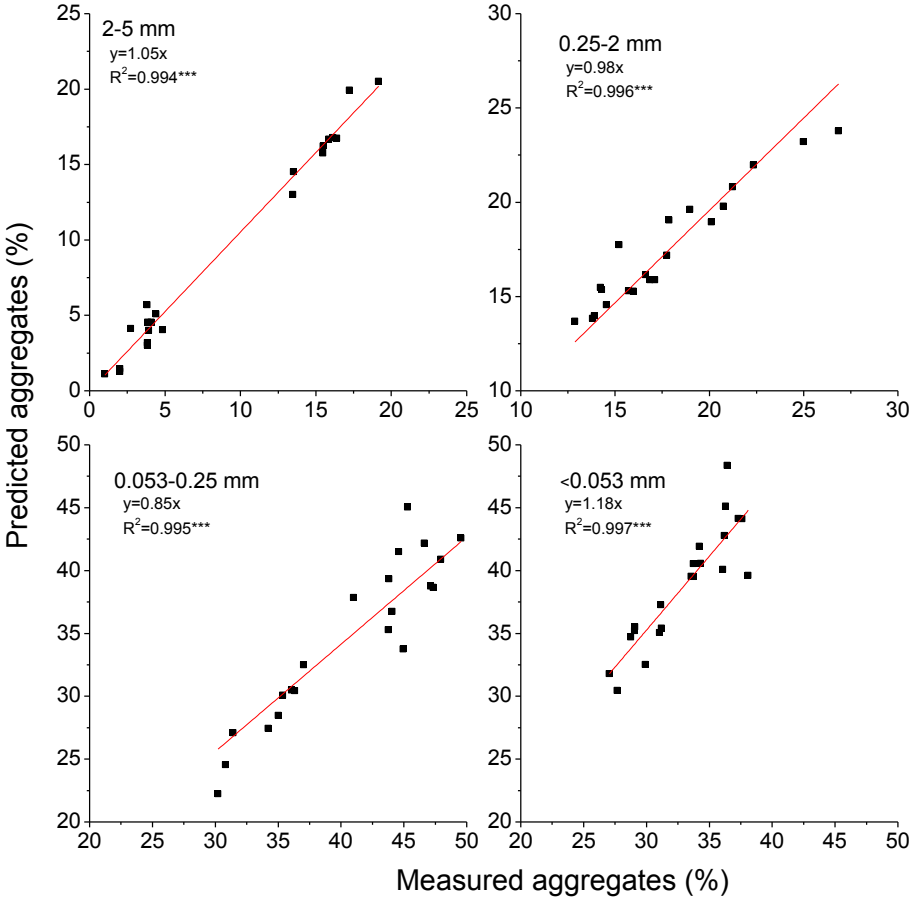

Fig. 10. The relationship between measured and predicted aggregates as defined in Equation (7).

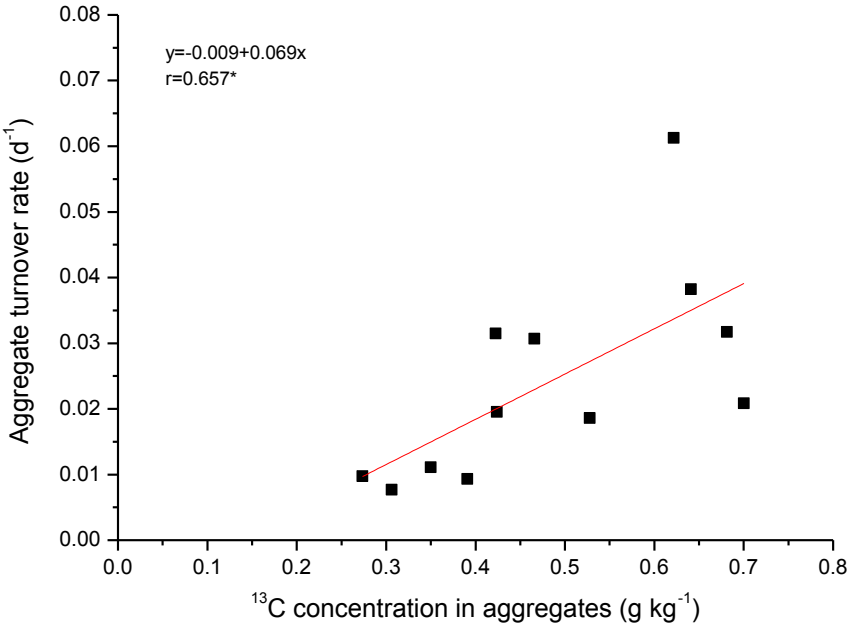

Fig. 11. The linear relationship between aggregate turnover rate and ^{13}C concentration in aggregates (n = 12).

3.6. Changes in aggregates in breakdown and buildup directions

Aggregate breakdown of different fractions is described using Equations (14)–(16) and buildup (formation) is described using Equations (17)–(19) (Fig. 12). In the breakdown direction the negative value means less aggregate disruption relative to the

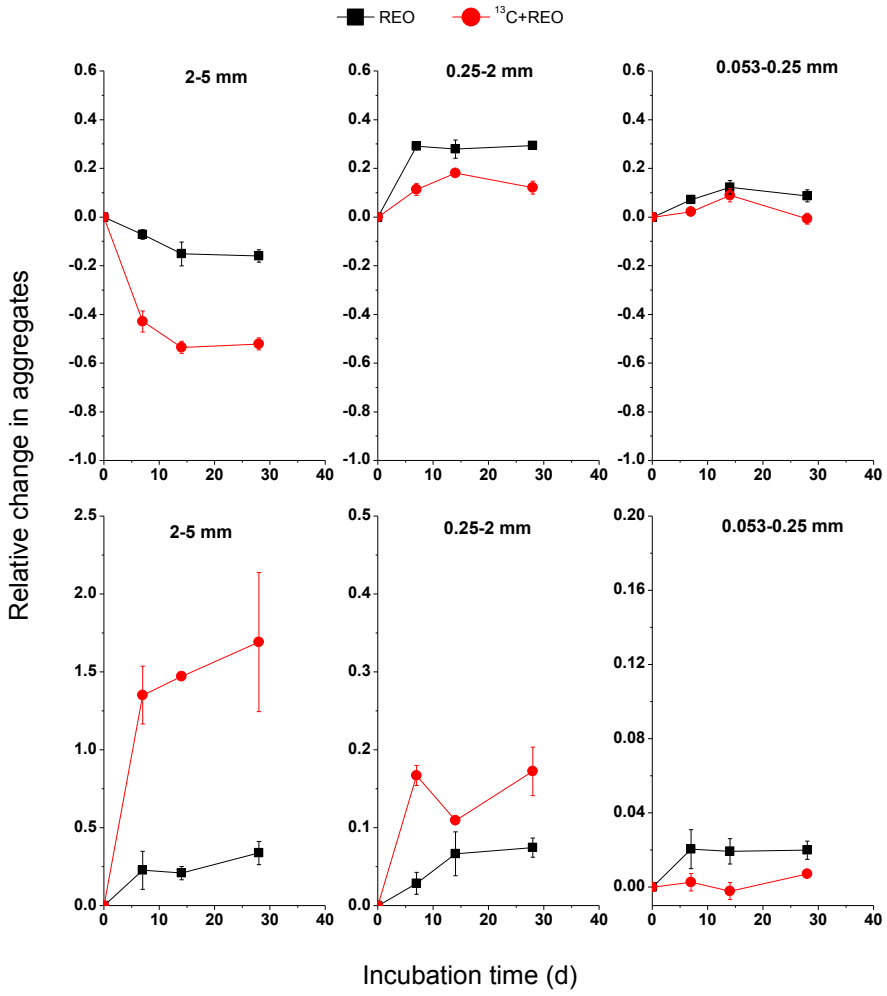

Fig. 12. Relative changes in aggregates in the breakdown direction as defined in Equations (14)–(16) (top) and in the buildup direction as defined in Equations (17)–(19) (bottom).

Table 2
Turnover time (day) for the four aggregate fractions with or without glucose addition. Different lowercase letters denote significant differences at $P < 0.05$ between sampling dates under the same treatment, and different captical letters denote significant differences at $P < 0.05$ between treatments on the same sampling date.

Treatments	Incubation time	2–5 mm	0.25–2 mm	0.053–0.25 mm	<0.053 mm
REO	7 d	103 ± 25 bA	23 ± 1 cB	69 ± 4 bA	47 ± 16 cA
	14 d	99 ± 31 bA	48 ± 6 bA	84 ± 11 bA	89 ± 28 bA
	28 d	179 ± 26 aA	87 ± 2 aB	186 ± 24 aA	171 ± 27 aA
^{13}C + REO	7 d	16 ± 2 cB	32 ± 3 cA	33 ± 4 cB	32 ± 1 bA
	14 d	26 ± 1 bB	48 ± 0 bA	52 ± 5 bB	94 ± 22 aA
	28 d	54 ± 3 aB	107 ± 6 aA	130 ± 9 aB	103 ± 9 aB

initial condition, while the positive value is a greater disruption. In the REO and ^{13}C + REO treatments, the amount of 2–5 mm aggregates increased but the other two fractions decreased over time as compared to the initial condition during the breakdown process (Fig. 12, top). The relative change showed an exponential decrease for 2–5 mm aggregates and an exponential increase for 0.25–2 mm aggregates. For the 0.053–0.25 mm aggregates, the exponential trend was not clear. The 0.25–2 mm aggregates showed a much greater breakdown proportion than 0.053–0.25 mm aggregates. Relative to the REO treatment, the glucose addition enhanced aggregate stabilization for 2–5 mm aggregates and reduced the breakdown of the other fractions significantly.

In the buildup direction, the amount of newly formed soil aggregates increased over the incubation time with or without ^{13}C-glucose addition, but this change decreased with decreasing aggregate size considerably (Fig. 12, bottom). The glucose addition increased the amount of new macroaggregates (0.25–2 mm and 2–5 mm) significantly relative to the REO treatment but decreased new microaggregates (0.053–0.25 mm). The amount of new 2–5 mm aggregates built up from the other three smaller fractions was 135% of the initial amount on day 7 incubation, up to 169% on day 28 incubation after glucose addition, whereas they were only by 23% and 28% at the same time in the REO treatment. The newly formed 0.25–2 mm aggregates, which were formed from <0.25 mm fractions, were 7.5% and 17% of the initial amount of this fraction on day 28 in the REO and ^{13}C + REO treatments,

respectively. The new 0.053–0.25 mm aggregates built up by < 0.053 mm fraction was only 0.7–2% of the initial amount at the end of incubation.

4. Discussion

4.1. REO as a tracer for aggregate turnover

A recovery of 84–106% for the four REOs after incubation (Table 1) was similar to the study (83.5–96.9%) of Zhang et al. (2001) in which REO-labelled aggregates were subjected to wetting and air-drying procedure, but greater than the recovery rates of 67–115% reported by De Gryze et al. (2006). In the study of De Gryze et al. (2006), they mixed REO as powder with the <250 μm aggregates. As compared to the method of mixing REO powder with aggregates directly, the wet mixing method of spraying REO and water onto the soil and then drying can significantly improve the immobility of REO and obtain a more homogeneous distribution in differently-sized aggregates (data not shown).

The close 1:1 line between measured and predicted aggregates (Fig. 10) supported De Gryze et al.'s (2006) findings that REOs are effective tracers of aggregate formation and breakdown dynamics. Like their study, we also found that REOs did not impact microbial activity (Fig. 3). Whilst REO was an effective tracer, there were limitations. The weaker relationship for 0.053–0.25 mm (slope = 0.85) and <0.053 mm (slope = 1.18) aggregates (Fig. 10) may be an experimental artefact due to the additional loss or gain of these two fractions during the wet sieving procedure, respectively.

4.2. Relation between new C distribution and aggregation

The exponential increase of aggregate stability (MWD) over time following ^{13}C-labelled glucose addition (Fig. 5) agreed with many previous studies that incubated soils for several weeks under controlled conditions (Watts et al., 2001; De Gryze et al., 2006) to over ten crop growing seasons in field conditions (Kay et al., 1988; Jastrow, 1996). Monnier's (1965) conceptual model of soil aggregation, however, predicts that the aggregate stability increases firstly and later decreases over time, as demonstrated in other experimental studies (Abiven et al., 2008; Mizauta et al., 2015). Although our data did not show a decrease in aggregate stability over time, the increase of aggregate stability agrees with the first portion of Monnier's model curve. This could be due to our short incubation time or the variability between aggregate stability and organic matter input. Abiven et al. (2009) reviewed 48 sets of data published since the 1940s and found inconsistent trends between different studies. Certainly, a clear and general relationship between the dynamics of aggregate stability and its interaction with the decomposition of organic matter requires more studies in different ecosystems.

Greater ^{13}C concentration in 2–5 mm and 0.25–2 mm fractions compared to the <0.25 mm fraction (Fig. 7) indicates that the new C was more readily accumulated in macroaggregates than in microaggregates. This is likely due to the rate of glucose movement into macroaggregates through large pores that are available in comparison to microaggregates (Chenu et al., 2001; Zhou et al., 2013). There may be greater loss of ^{13}C during wet sieving for <0.25 mm aggregates as well, due to the greater surface area to volume ratio and shorter transport pathways compared to larger aggregates (Fig. 6). By 28 days incubation, however, ^{13}C losses by wet sieving were minimal.

According to aggregate hierarchy model (Tisdall and Oades, 1982), greater new C in macroaggregates results from the binding of smaller aggregates by additional C. The ^{13}C-glucose joined the newly formed macroaggregates as a binding agent in the ^{13}C + REO treatment (Fig. 9). On the other hand, the new C in macroaggregates decomposed faster over time than in the microaggregates (Fig. 7). A variety of processes could drive slower decomposition of ^{13}C in microaggregates including localised aeration status, native C quality, microbial community structure and possibly physical protection (Chenu et al., 2001; Cosentino et al., 2006). The less physical protection of C in macroaggregates than microaggregates agrees with many studies (Puget et al., 2000; Six et al., 2002; Tian et al., 2015). Therefore, the double-labelled method in this study clearly shows that the new C preferentially formed macroaggregates but persisted over a shorter time than in microaggregates. Studies with a greater range of organic substrates, such as a ^{13}C labelled plant residues, would evaluate physical protection processes in greater detail.

4.3. Dynamic of aggregates: breakdown, stabilization and formation processes

The three processes of aggregate dynamics: formation, stabilization and breakdown, have been mentioned in many studies (Oades, 1993; Degens, 1997; De Gryze et al., 2005). Six et al. (2004) reviewed the biotic and abiotic factors for aggregate formation and breakdown mechanisms, but aggregate stabilization processes are multi-faceted and difficult to disentangle. In this study, we defined aggregate stabilization as the increasing resistance of aggregates to disruption over time under no additional input or stabilizing organic materials. Aggregate stabilization therefore indicates that aggregate disruption decreases over time. The negative values of the relative change in 2–5 mm aggregates over time with or without ^{13}C-glucose addition in the breakdown direction (Fig. 12) indicates progressively less breakdown and hence stabilization of this fraction compared to the initial condition. Kemper and Rosenau (1986) pointed out that the stability of aggregates can increase with storage time. Denef et al. (2001) also reported macroaggregates become more resistant to slaking with time after two drying and wetting cycles. In addition to microbial decomposition of organic compounds altering aggregate bonding properties over time, age hardening may further increase bond strength through greater capillary bonding stresses (Utomo and Dexter, 1981; Dexter, 1988) and physiochemical cementation between organic C and mineral oxides (von Lützow et al., 2006) that evolve over time as soil structure develops.

According to the distribution of REO tracers in different aggregate size fractions, the new C input decreased the breakdown of all sizes of aggregates and increased their formation rate (Figs. 8 and 9). Our results show that aggregates preferred a transfer to form a portion of the neighbouring fraction in both the breakdown and the formation directions. This does not agree with De Gryze et al. (2006) who found that under breakdown most of the portions of all aggregate size fractions were transferred into the <0.053 mm fraction. This difference may be soil specific and caused by the poorer stability of artificial macroaggregates in their study. In the formation direction, the newly formed aggregates exponentially increased with time, with larger aggregates forming faster than smaller ones (Fig. 12). Therefore, REO tracers do not only track aggregate transfer paths but also separate aggregate dynamics into breakdown, stabilization and formation processes.

4.4. Aggregate turnover and modelling

Although aggregate turnover forms the basis of a very large number of studies, an in-depth analysis of the transfer pathways is rare (Staricka et al., 1992; Plante et al., 1999, 2002; Plante and McGill, 2002b; De Gryze et al., 2006). Tracking aggregate

turnover pathways is difficult and can only be postulated from changes in aggregate stability unless tracers are used. Our results show that aggregate turnover time increased with a decrease in aggregate size (Table 2), similar to the results of De Gryze et al. (2006). However, the aggregate turnover times we found were 54–130 days, compared to 11–38 days reported by De Gryze et al. (2006) and 4–33 days reported by Plante et al. (2002). De Gryze et al. (2006) and Plante et al. (2002) added approximately 2 g maize straw 100 g^{-1} soil, whereas we added much more easily decomposed glucose. Using our proposed Eq. (12), the turnover times of A, B, C and D aggregate fractions in the study of De Gryze et al. (2006) were 32, 525, 33 and 35 days, respectively, after one week incubation. This shows similar microaggregate turnover and slower macroaggregate turnover rates to our study (Table 2).

The significantly linear relationship between aggregate turnover rate and ^{13}C concentration indicates that ^{13}C addition enhanced aggregate turnover (Fig. 11). Thus, our results provide new evidence that the C input caused macroaggregate turnover to be faster than in microaggregates, which is in accordance with many other studies that have not been able to track aggregate turnover directly through the use of tracers (Jastrow, 1996; Puget et al., 2000; Coq et al., 2007).

In this study, we proposed a first order kinetic model (Eq. (25)) based on the relative change in each aggregate fraction. Under controlled conditions (e.g. constant soil temperature and moisture), the decomposition of soil organic matter generally follows a first order decay (Jastrow, 1996; Berg, 2014; Castellano et al., 2015). The exudates of organic matter decomposition and microbial biomass are major binding agents in aggregation. Thus, the first order growth model for aggregate formation and stabilization corresponds to the dynamics of soil organic matter. Segoli et al. (2013) also pointed out a similar pattern between an aggregate dynamic model (AggModel) and soil organic matter dynamics, where both could be described by the first order model. On the other hand, the aggregate breakdown process after cultivation also followed a first order decay model as reported by Low (1972) and simulated later by Kay et al. (1988). Fuller and Goh (1992) found that the amount of clay sized aggregates produced as a function of applied sonic energy also followed a first order decay model. Thus, the first order kinetic model, summed up from the first order growth model for aggregate formation and stabilization and the first decay model for aggregate breakdown, describes aggregate dynamics well. The model proposed in our study is based on the short-term controlled conditions. It cannot describe the Monnier's (1965) model that aggregate stability has an increasing trend immediately after organic inputs and then a decrease as the decomposition of organic substances slows. However, the aggregate stability in Monnier's model sums up the formation and breakdown aggregate dynamics. This will be investigated in the future by extending our combined approach of using labelled C and REO tracers to different ecosystems under both laboratory-based studies and field conditions. Different labelled C sources will also be investigated, including materials with different levels of recalcitrance and plant residues.

5. Conclusions

Our combined approach of ^{13}C and REO labelling of soil aggregates effectively traced the interaction between C and aggregate dynamics in soil. This was shown by the high recovery of REOs during aggregate fractionation and the 1:1 relationship between measured and predicted aggregates. The aggregate stability increased greatly immediately after C input as glucose and then slowed down with the further decomposition of this added substrate. The new C accumulated more in macroaggregates (>0.25 mm) but decomposed faster than that in microaggregates (0.053–0.25 mm) and silt and clay sized aggregates (<0.053 mm). Another major advancement was a predictive model of the effect of incubation time on aggregate dynamics and aggregate turnover. Simultaneous transfer pathways of C and soil aggregates enabled with dual tracers offers considerable opportunity for further research exploring soil stability, C mineralization and C physical protection. In developing the approach we only studied short-term impacts using a labile C substrate and a highly weathered Acrisol soil dominated by 1:1 clay minerals and iron oxides. There is considerable potential to apply this approach to study a broader range of soils, ecosystems and incorporated organic matter quality from laboratory to field conditions.

Acknowledgements

This work was granted by the China-UK jointed Red Soil Critical Zone project from National Natural Science Foundation of China (NSFC: 41571130053, 41371235) and from Natural Environmental Research Council (NERC: Code: NE/N007611/1).

Appendix A. Supplementary data

Supplementary data related to this article can be found at http://dx.doi.org/10.1016/j.soilbio.2017.02.002.

References

Abiven, S., Menasseri, S., Angers, D.A., Leterme, P., 2008. A model to predict soil aggregate stability dynamics following organic residue incorporation under field conditions. Soil Science Society of America Journal 72, 119–125.
Abiven, S., Menasseri, S., Chenu, C., 2009. The effects of organic inputs over time on soil aggregate stability - a literature analysis. Soil Biology & Biochemistry 41, 1–12.
Bayon, G., Barrat, J.A., Etoubleau, J., Benoit, M., Bollinger, C., Revillon, S., 2009. Determination of rare earth elements, Sc, Y, Zr, Ba, Hf and Th in geological samples by ICP-MS after Tm addition and alkaline fusion. Geostandards and Geoanalytical Research 33, 51–62.
Berg, B., 2014. Decomposition patterns for foliar litter - a theory for influencing factors. Soil Biology & Biochemistry 78, 222–232.
Castellano, M.J., Mueller, K.E., Olk, D.C., Sawyer, J.E., Six, J., 2015. Integrating plant little quality, soil organic matter stabilization, and the carbon saturation concept. Global Change Biology 21, 3200–3209.
Chiang, P.N., Wang, M.K., Chiu, C.Y., King, H.B., Hwong, J.L., 2004. Changes in the grassland-forest boundary at Ta-Ta-Chia long term ecological research (LTER) site detected by stable isotope ratios of soil organic matter. Chemosphere 54, 217–224.
Chenu, C., Hassink, J., Bloem, J., 2001. Short-term changes in the spatial distribution of microorganisms in soil aggregates as affected by glucose addition. Biology and Fertility of Soils 34, 349–356.
Coq, S., Barthès, B.G., Oliver, R., Rabary, B., Blanchart, E., 2007. Earthworm activity affects soil aggregation and organic matter dynamics according to the quality and localization of crop residues - an experimental study (Madagascar). Soil Biology & Biochemistry 39, 2119–2128.
Cosentino, D., Chenu, C., Le Bissonnais, Y., 2006. Aggregate stability and microbial community dynamics under drying-wetting cycles in a silt loam soil. Soil Biology and Biochemistry 38, 2053–2062.
De Gryze, S., Six, J., Brits, C., Merckx, R., 2005. A quantification of short-term macroaggregate dynamics: influences of wheat residue input and texture. Soil Biology & Biochemistry 37, 55–66.
De Gryze, S., Six, J., Merckx, R., 2006. Quantifying water-stable soil aggregate turnover and its implication for soil organic matter dynamics in a model study. European Journal of Soil Science 57, 693–707.
Degens, B.P., 1997. Macro-aggregation of soils by biological bonding and binding mechanisms and the factors affecting these: a review. Australian Journal of Soil Research 35, 431–459.
Denef, K., Six, J., Bossuyt, H., Frey, S.D., Elliott, E., Merckx, R., Paustian, K., 2001. Influence of dry-wet cycles on the interrelationship between aggregate, particulate organic matter, and microbial community dynamics. Soil Biology & Biochemistry 33, 1599–1611.
Dexter, A.R., 1988. Advances in characterization of soil structure. Soil & Tillage Research 11, 199–238.
Díaz-Zorita, M., Perfect, E., Grove, J.H., 2002. Disruptive methods for assessing soil structure. Soil & Tillage Research 64, 3–22.
Elliott, E.T., 1986. Aggregate structure and carbon, nitrogen, and phosphorus in native and cultivated soils. Soil Science Society of America Journal 50, 627–633.
Fuller, L.G., Goh, T.B., 1992. Stability-energy relationships and their application to

aggregation studies. Canadian Journal of Soil Science 72, 453–466.
FAO, 2014. World Reference Base for Soil Resources. FAO, Rome.
Jastrow, J.D., 1996. Soil aggregate formation and the accrual of particulate and mineral-associated organic matter. Soil Biology Biochemistry 28, 665–676.
Kay, B.D., Angers, D.A., Groenevelt, P.H., Baldock, J.A., 1988. Quantifying the influence of cropping history on soil structure. Canadian Journal of Soil Science 68, 359–368.
Kemper, W.D., Rosenau, R.C., 1986. Aggregate stability and size distribution. In: Klute, A. (Ed.), Methods of Soil Analysis. Part. 1. 2nd, ASA and SSSA. WI., Madison, pp. 425–442.
Le Bissonnais, Y., 1996. Aggregate stability and assessment of soil crustability and erodibility: I. Theory and methodology. European Journal of Soil Science 47, 425–437.
Low, A.J., 1972. The effect of cultivation on the structure and other physical properties of grassland and arable soils (1945-1970). Journal of Soil Science 23, 363–380.
Mizauta, K., Taguchi, S., Sato, S., 2015. Soil aggregate formation and stability induced by starch and cellulose. Soil Biology & Biochemistry 87, 90–96.
Monnier, G., 1965. Action des matières organiques sur la stabilité structurale des sols. Thèse. Factulté des sciences de Paris.
Oades, J.M., 1993. The role of biology in the formation, stabilization and degradation of soil structure. Geoderma 56, 377–400.
Plante, A.F., Duke, M.J., McGill, W.B., 1999. A tracer sphere detectable by neutron activation for soil aggregation and translocation studies. Soil Science Society of America Journal 63, 1284–1290.
Plante, A.F., Feng, Y., McGill, W.B., 2002. A modeling approach to quantifying soil macroaggregate dynamics. Canadian Journal of Soil Science 82, 181–190.
Plante, A.F., McGill, W.B., 2002a. Intraseasonal soil macroaggregate dynamics in two contrasting field soils using labeled tracer spheres. Soil Science Society of America Journal 66, 1285–1295.
Plante, A.F., McGill, W.B., 2002b. Soil aggregate dynamics and the retention of organic matter in laboratory-incubated soil with differing simulated tillage frequencies. Soil & Tillage Research 66, 79–92.
Puget, P., Chenu, C., Balesdent, J., 2000. Dynamics of soil organic matter associated with particle-size fractions of water-stable aggregates. European Journal of Soil Science 51, 595–605.
Segoli, M., De Gryze, S., Dou, F., Lee, J., Post, W.M., Denef, K., Six, J., 2013. AggModel: a soil organic matter model with measurable pools for use in incubation studies. Ecological Modelling 263, 1–9.
Six, J., Bossuyt, H., De Gryze, S., Denef, K., 2004. A history of research on the link between (micro)aggregates, soil biota, and soil organic matter dynamics. Soil & Tillage Research 79, 7–31.
Six, J., Conant, R.T., Paul, E.A., Paustian, K., 2002. Stabilization mechanisms of soil organic matter: implications for C-saturation of soils. Plant and Soil 241, 155–176.
SPSS, 2004. SPSS 13.0 for Window. SPSS Inc., Chicago.
Stamati, F.E., Nikolaidis, N.P., Banwart, S., Blum, W.E.H., 2013. A coupled carbon, aggregation, and structure turnover (CAST) model for topsoils. Geoderma 211–212, 51–64.
Staricka, J.A., Allmaras, R.R., Nelson, W.W., Larson, W.E., 1992. Soil aggregate longevity as determined by the incorporation of ceramic spheres. Soil Science Society of America Journal 56, 1591–1597.
Tian, J., Pausch, J., Yu, G., Blagodatskaya, E., Gao, Y., Kuzyakov, Y., 2015. Aggregate size and their disruption after 14C-labeled glucose minerlization and priming effect. Applied Soil Ecology 90, 1–10.
Tisdall, J.M., Oades, J.M., 1982. Organic matter and water-stable aggregates in soils. Journal of Soil Science 33, 141–163.
Utomo, W.H., Dexter, A.R., 1981. Age hardening of agricultural top soils. Journal of Soil Science 32, 335–350.
von Lützow, M., Kögel-Knabner, I., Ekschmitt, K., Matzner, E., Guggenberger, G., Marschner, B., Flessa, H., 2006. Stabilization of organic matter in temperate soils: mechanisms and their relevance under different soil conditions - a review. European Journal of Soil Science 57, 426–445.
Watts, C.W., Whalley, W.R., Longstaff, D.J., White, R.P., Brooke, P.C., Whitmore, A.P., 2001. Aggregation of a soil with different cropping histories following the addition of organic materials. Soil Use and Management 17, 263–268.
Zhang, X.C., Friedrich, J.M., Nearing, M.A., Norton, L.D., 2001. Potential use of rare earth oxides as tracers for soil erosion and aggregation studies. Soil Science Society of America Journal 65, 1508–1515.
Zhou, H., Peng, X., Perfect, E., Xiao, T.Q., Peng, G.Y., 2013. Effects of organic and inorganic fertilization on soil aggregation in an Ultisol as characterized by synchrotron based X-ray micro-computed tomography. Geoderma 195–196, 23–30.
Zibilske, L.M., 1994. Carbon mineralization. In: Weaver, R.W., Angle, S., Bottomley, P., Bezdicek, D., Smith, S., Tabatabai, A., Wollum, A. (Eds.), Methods of Soil Analysis, Part 2, Microbiological and Biochemical Properties. Soil Science Society of America Book Series, vol. 5. Soil Science Society America Inc., Madison, pp. 835–864.